

# Understanding the Molecular Profile of the Lateral Parafacial Region

# UConn

Olivia Crawford, Daniel Mulkey

Physiology & Neurobiology, University of Connecticut

## Background

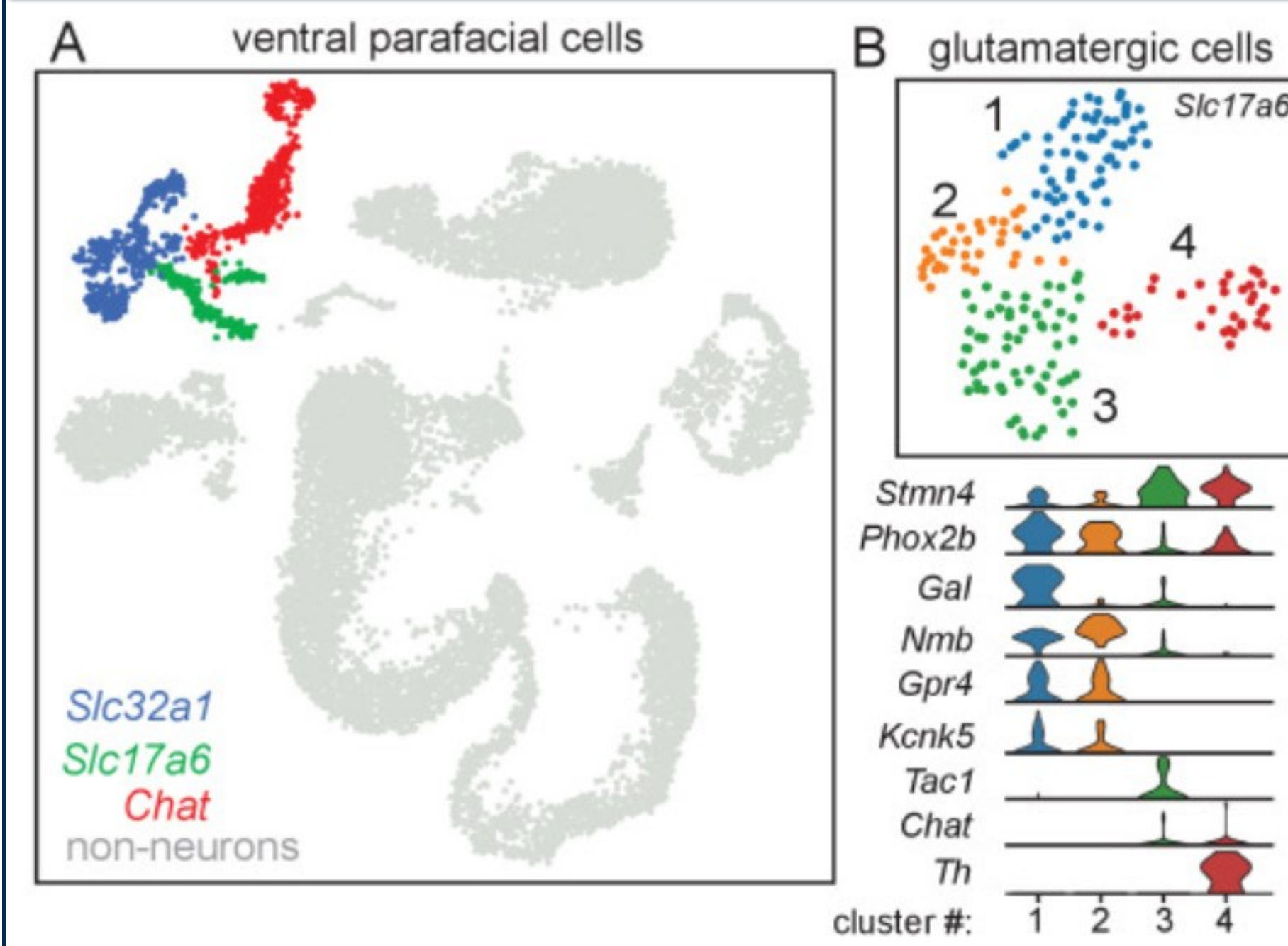


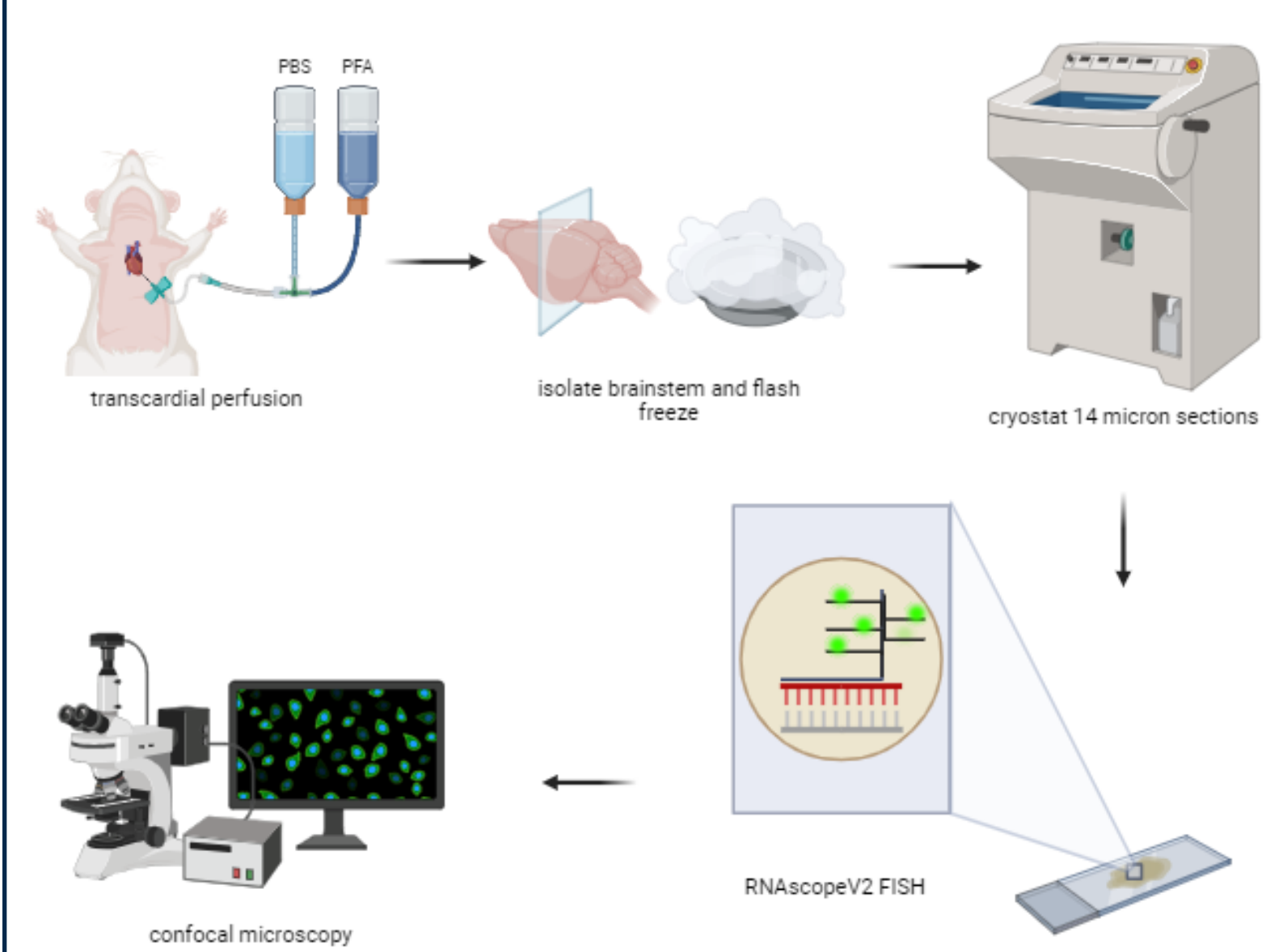
**Figure 1: RNA-seq data supports unique genetic identity of pFL neurons**  
A. T-distributed stochastic neighbor embedding (t-SNE) plot of the ventral parafacial single-cell transcriptome. Non-neurons were identified based on the lack of expression of Snap25, Syp, Tubb3, and Elavl1. Expression of Slc32a1, Slc17a6, and Chat was used for sub-cluster analysis of GABAergic, glutamatergic, and cholinergic neurons respectively.  
B. UMAP plot depicting four sub-clusters of glutamatergic, Slc17a6-expressing, neurons and corresponding violin plots showing cluster-specific differential gene expression. redrawn from<sup>6</sup>

Breathing consists of three stages; inspiration, post-inspiration, and expiration. Each stage has a proposed neural component that dictates their activity. In regards to expiration, there is both a passive and an active component, where the balance between the two is dictated by metabolic need. High levels of CO<sub>2</sub> or H<sup>+</sup> signal the recruitment of accessory abdominal muscles to increase pulmonary ventilation and contribute to metabolic homeostasis.

Due to both inspiration and expiration being influenced by changes in metabolism, it was thought that the retrotrapezoid nucleus (RTN) mediated both these stages of breathing<sup>2,3</sup>. However, recent work has shown that the RTN and its anatomical neighbor, the lateral parafacial (pFL) region, develop independently with different transcription factor requirements<sup>4,5</sup>, indicating that these two regions are functionally discrete. Although glutamatergic neurons in the pFL are thought to regulate active expiration<sup>1</sup>, unique genetic markers of this population remain unknown.

Previous work in the Mulkey Lab aimed at identifying factors that may be differentially expressed in the pFL compared to the RTN<sup>5,6</sup>. With the use of single-cell RNA sequencing (RNA-seq), they were able to identify four clusters of glutamatergic neurons in the RTN/pFL anatomical area. Clusters 1 and 2 contain expression of known markers of RTN chemosensitive neurons, including Phox2b, Neuromedin B (Nmb), Gpr4, and Kcnk5<sup>6,7,8</sup> (Fig. 1B). Cluster 4 has been identified to be sympathetic C1 catecholamine neurons that regulate blood pressure, and are therefore of uninterest. However, cluster 3 contains Phox2b, but lacks important pH sensing mechanisms that are present in the RTN clusters. Additionally, they uniquely express tachykinin 1 (Tac1) (Fig. 1B), and proenkephalin (PENK) (data not shown). We consider cluster 3 to be a leading pFL candidate, and therefore this project aimed to confirm these results through fluorescent in-situ hybridization (FISH) to visualize the presence of RNA transcripts assumed to be pFL markers (Tac1 and PENK) against known markers of the RTN (Gpr4, Kcnk5, and Nmb), with the hope of visualizing differential expression in these two anatomical regions.

## Materials and Methods



**Tissue Prep:** male juvenile (P21-24) wild type C57BL/6 mice were anesthetized (ketamine, 75 mg kg<sup>-1</sup>; xylazine, 5 mg kg<sup>-1</sup>; I.P.). Following the absence of response to a firm toe pinch, they were perfused transcardially with 4% paraformaldehyde-0.1 M phosphate buffer. Brains were removed and then fresh frozen by immersing them in dry ice and covering them with OCT (optimal cutting temperature) compound. Stored in -80°C until further processing.  
**Cryostat:** 14-micron sections, placed onto SuperFrost Plus slides (Fisher, Cat No. 12-550-15) and stored in -20°C until further processing.  
**RNAscopeV2:** remove slides from storage in -20°C and follow the step-by-step staining protocol outlined in the RNAscope Multiplex Fluorescent Assay (Advanced Cell Diagnostics).

**Confocal Imaging:** confocal images of FISH experiments were obtained using the Nikon AXR confocal. Confocal image files containing image stacks were uploaded into ImageJ and analyzed to determine the percentage colocalization of mRNA transcripts.

## Results

### PENK May be a Unique Marker of the pFL

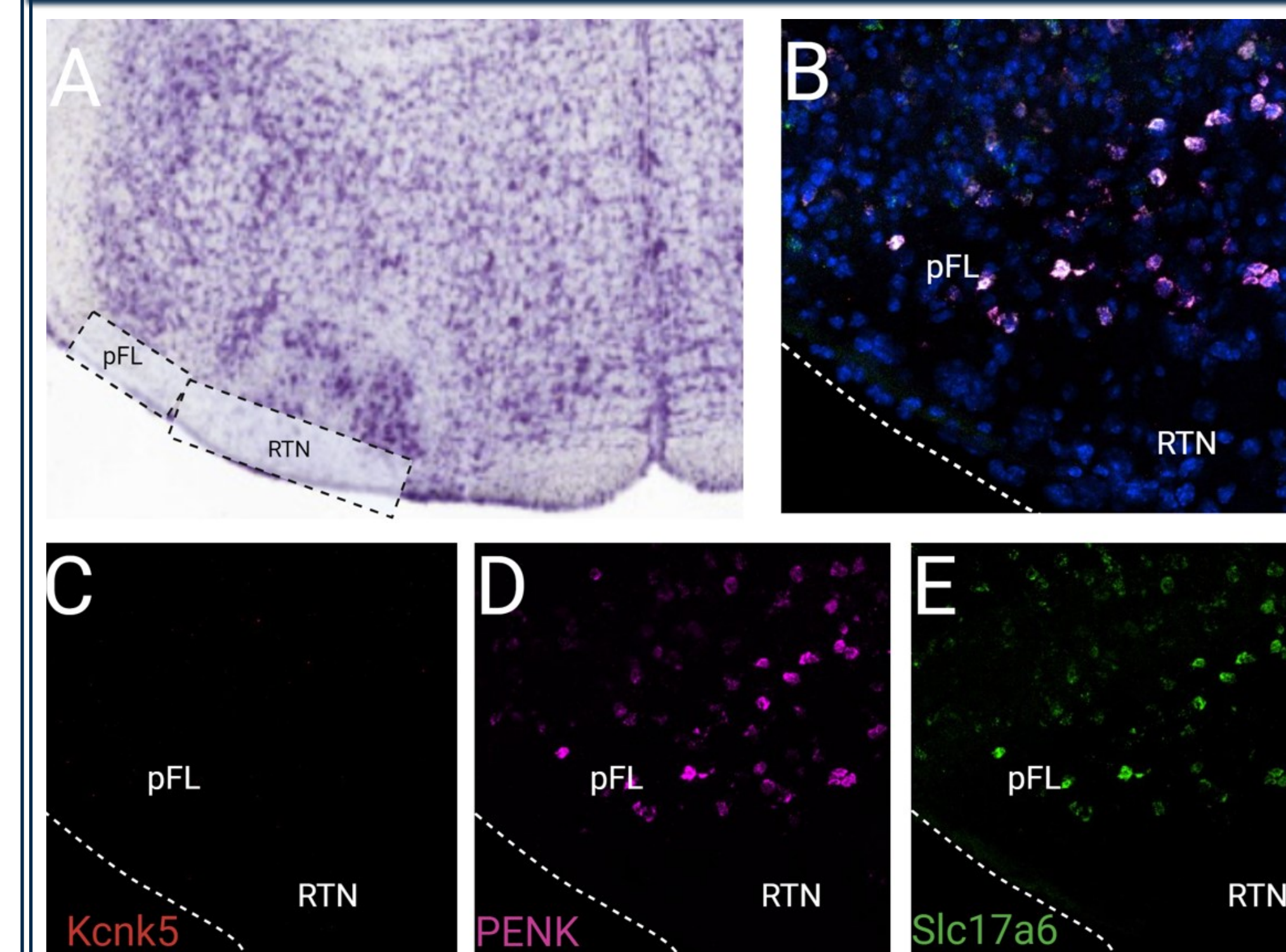


**Figure 2: PENK signal is restricted to the pFL region**  
A. mouse medulla<sup>10</sup> orienting the anatomical locations of the RTN and the pFL (nucleus), Kcnk5, PENK, and Slc17a6 with anatomically defined pFL and RTN locations  
B. merged image of representative coronal section of the medulla stained for DAPI (nucleus), Kcnk5, PENK, and Slc17a6 with anatomically defined pFL and RTN locations  
C. Kcnk5 signal does not meet threshold puncta amount; presence of at least five punctate fluorescent dots accompanying a nucleus labeled by 4',6-diamidino-2-phenylindole (DAPI)  
D. PENK expression localized to the pFL  
E. Slc17a6 expression localized to the pFL, with perfect colocalization

PENK expression was detected in the pFL area but not in the RTN. A minimum of five puncta were used as a threshold for what was considered a positive signal. The undetectable signal of Kcnk5 (Fig. 2B) raises concern about the efficiency of the probe used (Fig. 1B). Contrary to our expectation, the Slc17a6 signal was found in a discrete cluster in the pFL area, not in the RTN (Fig. 2E). This raises concern on the validity of Slc17a6 expression given our molecular data (Fig 1) and prior literature (Fig. 3B) shows robust expression in the RTN. Lack of Slc17a3 expression in the RTN suggests the Slc17a3 signal observed in the green channel (Fig 2E) is actually bleedthrough from PENK expression in the far red channel (Fig 2D). To quantitatively verify this, I calculated the manders' overlap coefficient. This analysis includes two variations, M1 and M2, which quantifies the fraction of fluorescence from channel 1 that is colocalized with channel 2 for M1, and vice versa for M2. Values range from 0 to 1, where 0 indicates no overlap between the channels, and 1 indicates a perfect colocalization between the two channels, and can signify bleed through. The results of this analysis comparing "channel 1" Slc17a6 and "channel 2" PENK gave an M1 of 0.9499 and M2 of 1.000 (Fig. 4C), indicating that the fluorescence in either of the channels is an artifact of the other's expression. Along with the fact that the Slc17a6 expression should be seen in areas where it is not, it leads me to believe that the PENK expression seen is real and Slc17a6 is an artifact of it, and not the other way around.

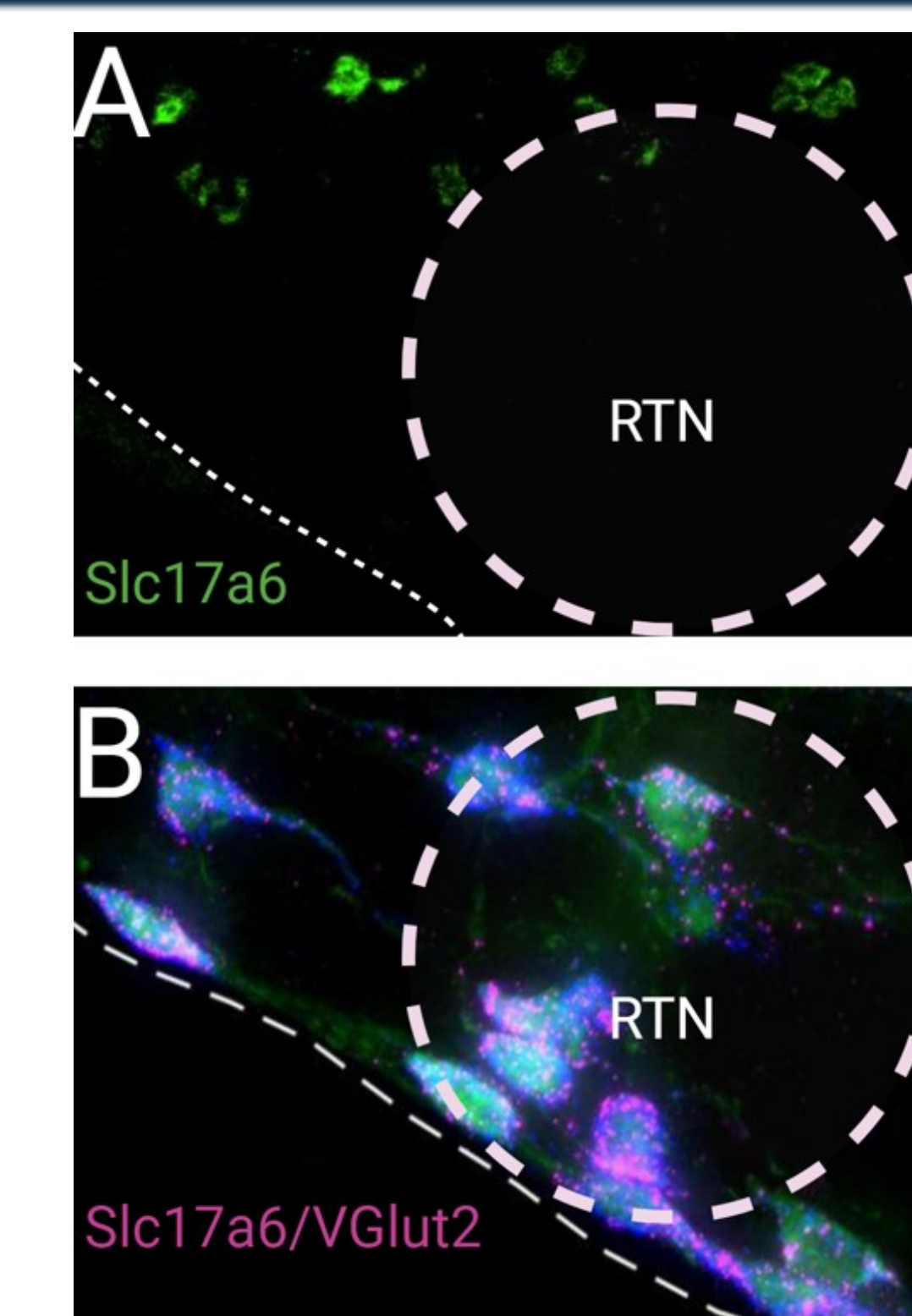


**Figure 3: Unable to confirm PENK labeled cells are glutamatergic**  
A. Slc17a6 mRNA expression absent in the RTN of mouse brain  
B. Slc17a6 (VGlut2) mRNA expression in the RTN of mouse brain, taken from<sup>11</sup>

### RNAscopeV2 Protocol has Bleedthrough Issues

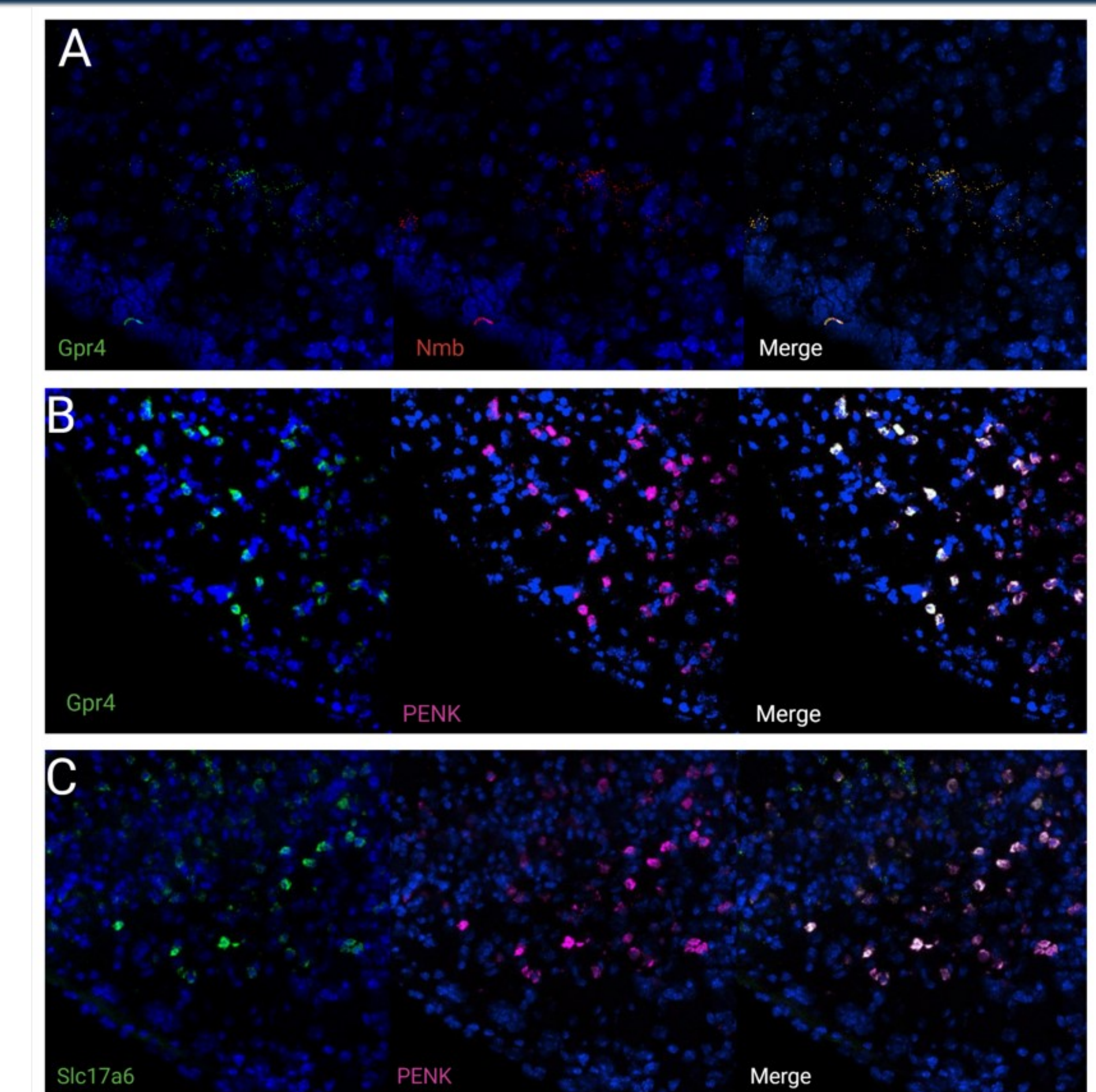
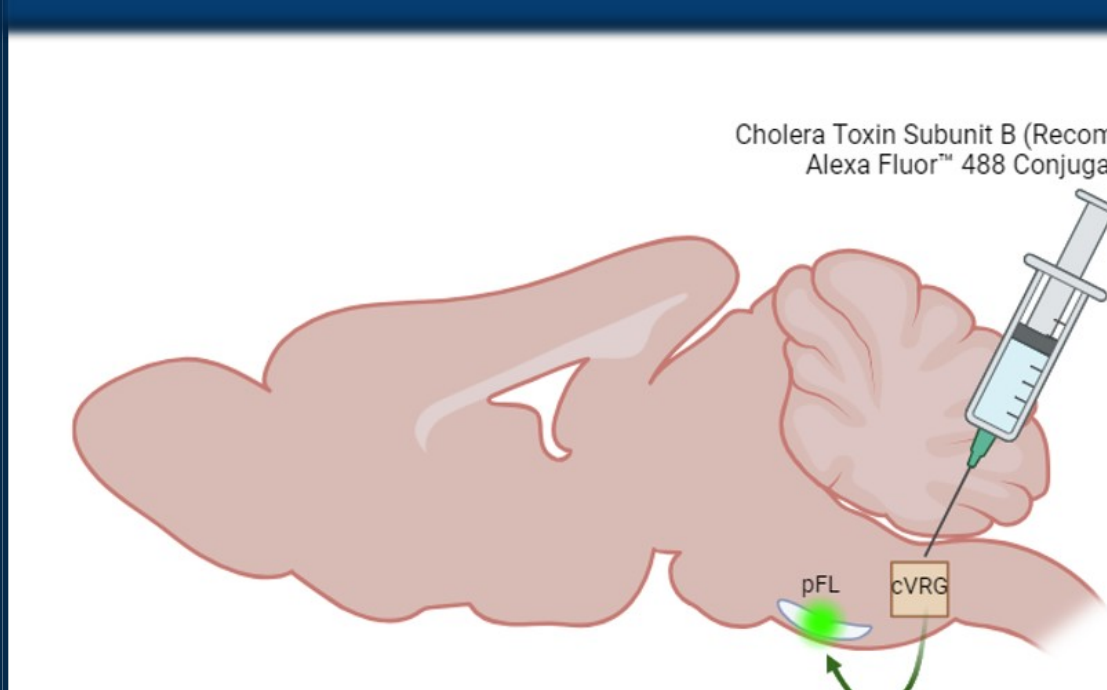


**Figure 4: RNAscopeV2 protocol has bleedthrough issues**  
A. Gpr4 and Nmb expression; manders' overlap coefficient for channel 1 (M1) of 0.9269 and manders' overlap coefficient for channel 2 (M2) of 0.9933  
B. Gpr4 and PENK expression M1 of 1.000 and M2 of 1.000  
C. Slc17a6 and PENK expression M1 of 0.9499 and M2 of 1.000

Although PENK appears to be expressed in the pFL, our results raise concerns on the efficiency and specificity of our in-situ hybridization assay. Manders' overlap coefficient comparing "channel 1" Gpr4 and "channel 2" Nmb resulted in M1 = 0.9269 and M2 = 0.9933 (Fig. 4A). Between Gpr4 and PENK, an M1 and M2 of 1.000 was found (Fig. 4B). As touched on, the comparison between Slc17a6 and PENK came to an M1 of 0.9499 and M2 of 1.000 (Fig. 4C). The levels of overlap between the channels is above physiological significance, and lends itself to bleedthrough between channels or artifact, rather than colocalization of two separate mRNA probe signals

## Future Directions



Given the lack of success using FISH, we hope to pivot to a new technique utilizing the anatomy of the mechanism behind active expiration. It is thought that the pFL projects to the caudal ventral respiratory group (cVRG)<sup>9</sup>, a group of expiratory pre-motor neurons. We will inject the cVRG with a retrograde tracer, Cholera Toxin Subunit B (CTB), which has been recombinant with Alexa Fluor™ 488 so that it will fluoresce green. We will then sacrifice the mice two weeks post-injection for subsequent cryostat and confocal imaging. Given that the injection is specific to the cVRG and the proposed anatomical pathway is correct, we expect to see green fluorescence in the pFL. With this, we hope to use immunohistochemistry (IHC) to visualize the co-localization of Tac1 and/or PENK in the pFL, along with visualizing the lack of co-localization with factors specific to the RTN, such as Gpr4 or Kcnk5.

## References

- Huckstepp RTR, Cardoza KP, Henderson LE, and Feldman JL. Distinct parafacial regions in control of breathing in adult rats. *PLoS One* 13: e0201485, 2018.
- Guyenet PG, Stornetta RL, Souza G, Abbott SGB, Shi Y, and Bayliss DA. The Retrotrapezoid Nucleus: Central Chemoreceptor and Regulator of Breathing Automaticity. *Trends Neurosci* 42: 807-824, 2019.
- Mulkey DK, Stornetta RL, Weston MC, Simmons JR, Parker A, Bayliss DA, and Guyenet PG. Respiratory control by ventral surface chemoreceptor neurons in rats. *Nat Neurosci* 7: 1360-1369, 2004.
- Rose MF, Ren J, Ahmad KA, Chao HT, Klisch TJ, Flora A, Greer JJ, and Zoghbi HY. Math1 is essential for the development of hind-brain neurons critical for perinatal breathing. *Neuron* 64: 341-354, 2009.
- Cleary CM, James S, Maher BJ, and Mulkey DK. Disordered breathing in a Pitt-Hopkins syndrome model involves Phox2b-expressing parafacial neurons and aberrant Nav1.8 expression. *Nat Commun* 12: 5962, 2021.
- Cleary CM, Milla BM, Kuo FS, James S, Flynn WF, Robson P, and Mulkey DK. Somatostatin-expressing parafacial neurons are CO(2)/H(+) sensitive and regulate baseline breathing. *Elife* 10: 2021.
- Shi Y, Sobrinho CR, Soto-Perez J, Milla BM, Stornetta DS, Stornetta RL, Takakura AC, Mulkey DK, Moreira TS, and Bayliss DA. 5-HT7 receptors expressed in the mouse parafacial region are not required for respiratory chemosensitivity. *J Physiol* 600: 2789-2811, 2022.
- Shi Y, Stornetta RL, Stornetta DS, Onengut-Gumuscu S, Farber EA, Turner SD, Guyenet PG, and Bayliss DA. Neuromedin B Expression Defines the Mouse Retrotrapezoid Nucleus. *J Neurosci* 37: 11744-11757, 2017.
- Rosin DL, Chang DA, and Guyenet PG. Afferent and efferent connections of the rat retrotrapezoid nucleus. *J Comp Neurol* 499: 64-89, 2006.
- Watson C. The Mouse Nervous System. *Handb Clin Neurol* pp:398-423, 2012
- Guyenet PG, Bayliss DA. Central respiratory chemoreception. *Handb Clin Neurol* 188:37-72, 2022.